In-Situ Silver Nanoparticle Formation on Surface-Modified Polyetherimide Films

David E. Watson, Jack H.-G. Ng, Knut E. Aasmundtveit, *Member, IEEE*, and Marc P. Y. Desmulliez, *Senior Member, IEEE*

***Abstract*—This paper extends the scope of a novel process previously reported by the group for the hydrolysis and subsequent metallization of polyimide substrates to encompass polyetherimide. Silver nanoparticles are grown *in-situ* by chemical reduction of silver ions implanted in the substrate. Factors affecting the level of hydrolysis are investigated, with temperature of the hydrolyzing solution found to be the key factor. The presence of silver nanoparticles is also confirmed by X-ray diffraction.**

***Index Terms*—Flexible substrate, interconnections, ion exchange, metallization, micropatterning, packaging, polyetherimide (PEI), silver nanoparticles.**

I. Introduction

ELECTRONIC products with ever more complex and specialized functions are in increasing demand across industries as diverse as healthcare, environment, security, and manufacturing of consumer goods. Such relentless appetite for smarter, lighter, and smaller products has driven innovations in material science, device fabrication, assembly, and packaging technologies to lower costs. In that respect, alternative materials and means of production, such as those encountered in organic/plastic electronics, are the subject of intensive research, as this technology offers a large variety of dielectric, semiconductive, and conductive low-cost materials to realize functionalities approaching the performance of silicon-based devices [1]. One particular area of research receiving increasing attention covers methods for the metallization of polymers [2]–[6], with polyimide (PI) receiving particular attention [7]–[12] due to the excellent properties of this material that include strong resistance to temperature and chemicals, good mechanical strength [13], and biocompatibility [10], [14], allowing thereby its use in a wide range of applications.

Manuscript received August 29, 2013; revised February 13, 2014; accepted April 15, 2014. Date of publication April 17, 2014; date of current version July 2, 2014. This work was supported by the Engineering and Physical Sciences Research Council (EPSRC) and the Innovative electronics Manufacturing Research Centre through the Flagship Project Smart Microsystems, (FS/O1/02/10). This work was also supported by the EPSRC-funded projects USINN, (EP/K020250/1), SONOPILL (EP/K034537/1), and PHOTOBIOFORM (EP/L022192/1). The review of this paper was arranged by Associate Editor G. Ramanath.

D. E. Watson, J. H.-G. Ng, and M. P. Y. Desmulliez are with MIcroSystems Engineering Centre, Heriot-Watt University, Edinburgh EH14 4AS, U.K. (e-mail: D.E.Watson@hw.ac.uk; J.H.Ng@hw.ac.uk; M.Desmulliez@hw.ac.uk).

K. E. Aasmundtveit is with the Institutt for mikro- og nanoteknologi, Høgskolen Vestfold, 3184 Borre, Norway (e-mail: Knut.Aasmundtveit@hive.no).

Color versions of one or more of the figures in this paper are available online at http://ieeexplore.ieee.org.

Digital Object Identifier 10.1109/TNANO.2014.2318203

Another polymer material with potential suitability for direct metallization is polyetherimide (PEI). Similar to PI in terms of physical properties, it exhibits excellent dielectric properties over a range of temperatures, has high strength and modulus, high heat and radiation (UV and Gamma ray) resistance [15]–[18], and is also USP Class VI compliant, indicating its suitability for medical devices. PEI can be used in a variety of applications, with the most prevalent one being the fabrication of molded interconnect devices (MID) [19]. PEI was recently suggested as a potential candidate for ion-exchange substrate surface modification [17]. Ion-exchange methods offer a simple way to produce metal nanoparticles and metal-polymer composites, which could provide a quicker route involving fewer processing steps to realizing interconnects within MIDs or aid in the creation of 3-D circuit. The surface modification of imide-based polymers and the subsequent *in-situ* ion exchange requires hydrolysis of the polymer by a strong alkali, a well studied effect [8]. This paper here provides evidence that, although requiring more stringent parameters than PI due to its superior alkali resistance, the surface modification, ion-exchange, and metallic salt reduction method is also applicable to PEI, and therefore, PEI is a suitable substrate for metallization via the laser direct-writing process previously reported by the group [9], [20].

II. Experimental Details

75-μm-thick grade 1000B Ultem PEI sheets were obtained from Cadillac Plastics, U.K. All other chemicals were obtained from Fisher Scientific, U.K. and Acros Organic, U.K. Full factorial design Of experiments (DOE) analysis was undertaken with the aid of the software package Minitab, version 14, from Minitab Inc. Fourier transform infrared apectroscopy (FTIR) measurements were taken with a PerkinElmer Spectrum 100 FT-IR spectrometer in ATR mode. Field emission scanning electron microscopy (FESEM) imaging was carried out using a Quanta 3-D FEG from FEI Company, USA, and XRD measurements obtained in transmission mode were taken with a D8 Discover from Bruker Corporation, Germany, using X-ray wavelength $\lambda = 1.5418$ Å.

III. Preparation of PEI Films for Ion-Exchange

The comparable physical properties of PEI and PI are partly explained by their similar monomers as evidenced by the structural comparison of PEI and the widely known PI, PMDA-ODA, as shown in Fig. 1.

Both contain two imide groups (O=C–N–C=O), which are instrumental in the ion-exchange process described in this paper.

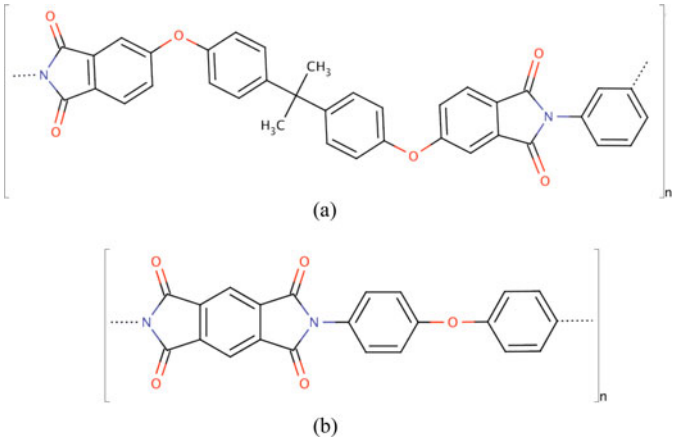

Fig. 1. Polyetherimide (a) and PMDA-ODA polyimide (b) repeat units.

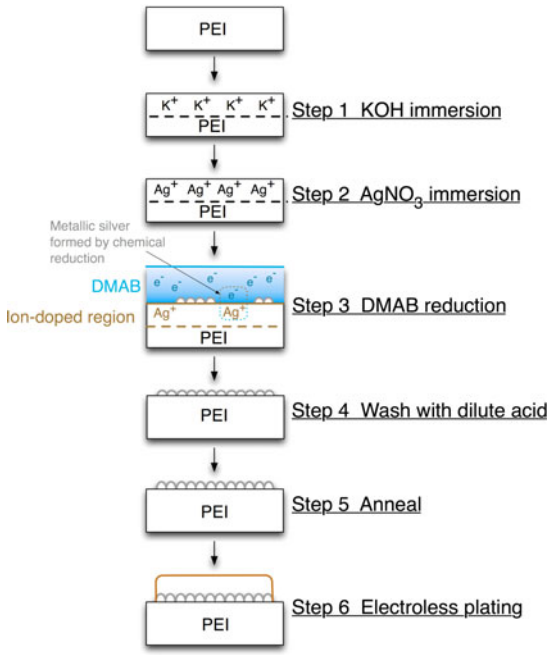

Fig. 2. Process steps for surface metallization and plating.

The procedure is similar to that described for PI/PMDA-ODA substrates [21] and is schematically described in Fig. 2. The substrate is initially rinsed with acetone then isopropanol to remove possible contaminants. It is then submerged in an ultrasonic bath of deionized (DI) water for a few minutes before being thoroughly rinsed with more DI water.

The immersion of the substrate in a potassium hydroxide (KOH) solution induces cleavage of the ring of the imide group; as a result a layer of potassium polyamate is formed at the surface of the substrate. After further rinsing in DI water, the substrate is then submerged in a silver nitrate $(AgNO_3)$ solution to form silver polyamate through potassium–silver ion exchange as indicated in Fig. 3(b). After further rinsing, the substrate is submersed in a dimethylamino-borane complex (DMAB) solution. This chemical is a very strong reducing agent and donates electrons to the silver ions to form silver particles, creating a silver seed layer of thickness suitable for subsequent electroless

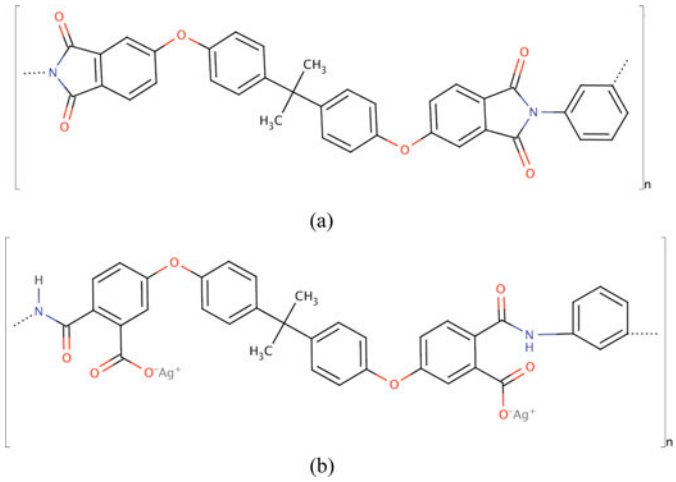

Fig. 3. (a) PEI, (b) silver polyamate.

plating. The substrate is then submerged in a dilute sulphuric acid solution to remove any unreacted silver ions before being placed in an oven to reform the imide bonds cleaved in the initial step. Finally, electroless plating may be carried out to attain the desired metal thickness.

Our preliminary tests found that the reported conditions for hydrolyzing PI, 1 molar KOH solution at 50 °C for 5 min, had a negligible effect on the PEI substrate, indicating it was less susceptible to alkaline attack than PI. A DOE was carried out to determine the optimum process parameters required to cleave the imide ring, such that the polymer is converted into polyamic acid as shown in Fig. 3. This full factorial DOE included temperature, concentration, immersion time, and type of alkali used as parameters. A "low" and a "high" value were chosen for the each continuous variable parameter—temperature, concentration, and time—while the "alkali-type" parameter was restricted to two discrete values; "sodium hydroxide" (NaOH) and "potassium hydroxide" (KOH). The various experimental parameter permutations can be found in the first five columns in Table I below.

After the ring cleavage step, all samples were submersed in a 0.1M $AgNO_3$ solution for 15 min at room temperature to exchange the potassium ions with their silver counterparts, resulting in the silver ions being electrostatically bonded to the PEI, as shown in Fig. 3(b). The silver ions were then chemically reduced to silver nanoparticles (NPs) by immersion in a 5-mM DMAB solution for 1 and 7 min, respectively. Following thorough rinsing in DI water, the substrate was submerged in 1% w/w sulphuric acid (H_2SO_4) for 5 min to remove any silver ions that did not react with DMAB. Reimidization was then carried out at 250 °C in air, nitrogen, or vacuum atmospheres for 30, 60, and 90 min.

IV. Results and Discussion

Table I shows the results of all experimental runs. The FTIR spectra for untreated PEI and for Run 16, the run, which showed the greatest change, are displayed in Fig. 4. The peaks at ∼1780 cm^{-1}, ∼1710 cm^{-1}, and ∼1370 cm^{-1} correspond to the C=O

TABLE I
RELATIVE IMIDE CONTENT OF MODIFIED PEI

Run number	Temp. (°C)	Conc. (M)	Time (min)	Alkali	1710 cm^{-1} C=O peak	1500 cm^{-1} benzene peak	1710 cm^{-1} peak to 1500 cm^{-1} peak ratio	Relative surface imide content (%)
Pristine	**-**	**-**	**-**	**-**	**2.88357**	**1.32336**	**2.17893**	**100**
1	50	5	20	NaOH	2.89947	1.33491	2.17203	99.6
2	80	5	20	NaOH	1.11149	1.28438	0.86500	39.7
3	50	15	20	NaOH	2.90063	1.33059	2.17996	100
4	80	15	20	NaOH	1.17719	1.31504	0.89517	41.1
5	50	5	40	NaOH	2.89517	1.32879	2.17880	100
6	80	5	40	NaOH	1.49238	1.33448	1.11832	51.3
7	50	15	40	NaOH	2.95424	1.34880	2.19027	100
8	**80**	**15**	**40**	**NaOH**	**0.35783**	**1.62320**	**0.22045**	**10.1**
9	50	5	20	KOH	3.13159	1.39502	2.24483	100
10	80	5	20	KOH	1.89049	1.37010	1.37010	62.9
11	50	15	20	KOH	2.79193	1.37519	2.03021	93.1
12	**80**	**15**	**20**	**KOH**	**0.17839**	**1.70683**	**0.10452**	**4.8**
13	50	5	40	KOH	3.21812	1.42541	2.25768	100
14	80	5	40	KOH	1.06623	1.37064	0.77791	35.7
15	50	15	40	KOH	2.28878	1.38691	1.65027	75.7
16	**80**	**15**	**40**	**KOH**	**0.01919**	**1.80382**	**0.01064**	**0.4**

Runs of particular interest highlighted in bold.

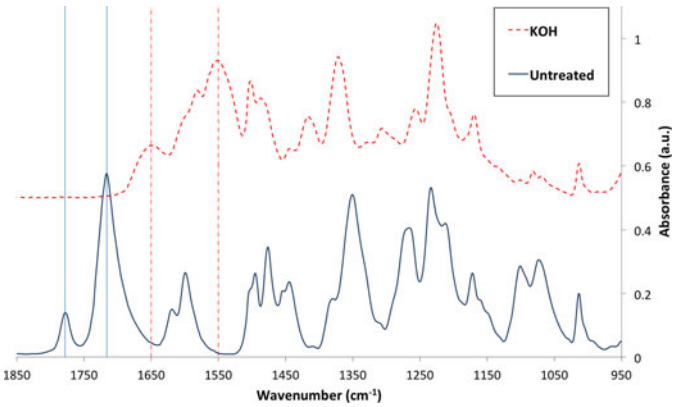

Fig. 4. FTIR-ATR spectra of untreated (lower, solid line), fully hydrolyzed PEI (upper, dashed line).

double bond asymmetric, C = O symmetric, and C-N-C imide ring stretches, respectively, and their presence confirms that there is complete imidization of the polymer chain. Peaks at 1650 cm^{-1} and 1550 cm^{-1} indicate amide I and II vibrations, respectively, which indicate that hydrolysis has taken place [9]. The amide groups are the newly created branches in the polymer chain where the metal ions bond to, as seen in Fig. 3(b).

Comparing the two graphs with respect to these peaks clearly shows the imide ring cleavage has occurred on the PEI substrate—the peaks for the untreated sample at ∼1780 cm^{-1} and ∼1710 cm^{-1} have disappeared, while peaks at ∼1650 cm^{-1} and ∼1550 cm^{-1} have appeared.

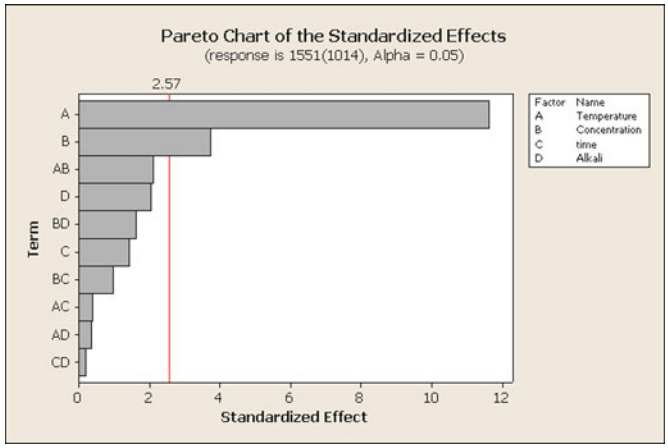

Fig. 5. Pareto chart of factors affecting imide ring cleavage, the greater the standardized effect of the parameter the greater the significance of that parameter (or parameter interactions).

To quantify the degree of hydrolysis, the magnitude of the most prominent imide peaks (1710 cm^{-1}) was divided by that of the peak at ∼1500 cm^{-1}, which is associated with one of the benzene ring breathing modes [22], [23], of which five exist in the PEI repeat unit. For more accurate comparison between samples, the spectra were normalized with respect to the peak at ∼1010 cm^{-1}, also known to indicate in-plane C–H benzene ring breathing [24]. The normalized peak ratio for each run was then divided by the normalized untreated peak ratio for untreated PEI to give an approximate percentage of imide content at the surface of the substrate as indicated in the last column of Table I. Most complete hydrolysis occurs either when all parameters are "high" (runs 8 and 16, respectively) or for run 12 where a high temperature, high KOH concentration, and low time have been used. Further evidence of hydrolysis is given by the formation of a carboxylic group, highlighted by peaks at ∼1650 cm^{-1} and ∼1550 cm^{-1} on FTIR spectra for these runs. As explained earlier, run 16 is shown on the uppermost graph in Fig. 4. The spectra for the other two runs are not presented here due to their high similarities with run 16. Both alkalis display broadly similar FTIR results, with KOH generally providing a higher surface imide content, as would be expected for this stronger base. It does appear however, that only runs with high temperature and high concentration parameters provided a thorough hydrolysis. The Pareto chart of standardized effects from the DOEs analysis in Fig. 5, and the standardized effects plot (not shown) clearly show that temperature (A), in Fig. 5, is the most important factor in the cleaving process, with concentration (B) also being somewhat significant, with a larger value having greater influence. The other single factors of time (C) and alkali type (D) were less significant. It should be noted however that the interaction between temperature and concentration (AB) enhances the hydrolysis reaction on top of the individual effects of each single factor.

80 °C appeared to be the threshold for significant degree of hydrolysis, using 15M concentration of alkali. On the basis of these results, a PEI hydrolysis regime of 15M KOH at 80 °C for

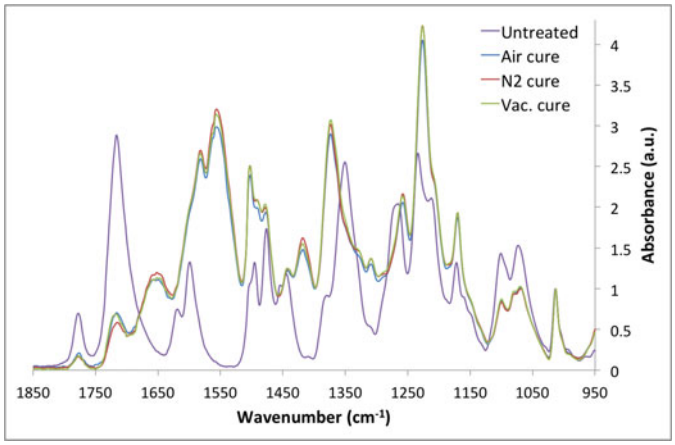

Fig. 6. FTIR spectra of PEI samples after the imide ring cleaving step treated for 90 min.

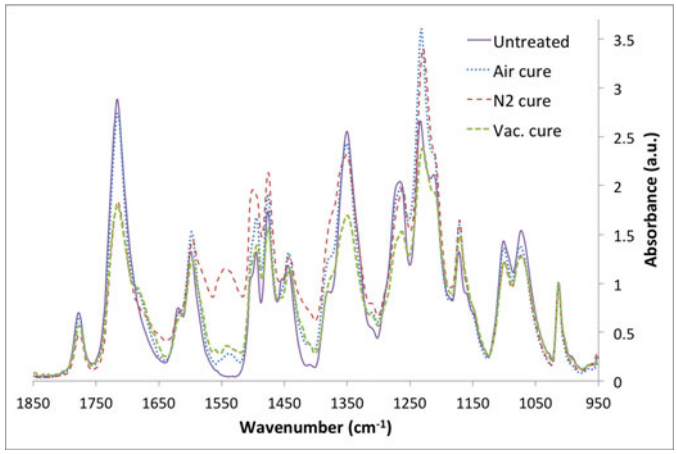

Fig. 7. FTIR spectra of PEI samples annealed for 90 min in different atmospheres after ion-exchange step.

the minimal treatment time of 20 min was chosen for the investigation and characterization of the subsequent process steps.

Effects of the reimidization process were then investigated by studying the annealing of the samples that had been treated in DMAB for 1 min. They were annealed at 250 °C in air or nitrogen at ambient pressure. Samples were treated for 30, 60, or 90 min in each of these atmospheres. The heating regime consisted of a 20-min heating ramp from room temperature to 250 °C, where the temperature was held for either 30, 60, or 90 min before a cooling down period of approximately 15 min to bring it back to under 100 °C. The samples were also annealed under vacuum but the heating regime differed slightly from the runs above due to the length of time the vacuum oven took to vary the temperature. The samples were placed in the vacuum oven at 160 °C, from which it took approximately 30 min to reach the desired temperature. Similarly, the cooling ramp of 15 min. for the air and nitrogen samples was not possible to achieve while maintaining a vacuum, and so samples were removed directly from the oven with no extended cooling down period.

Samples were annealed after different stages of the process to assess substrate behavior with and without silver particles or ions being present. More precisely, the annealing step was carried out after the hydrolysis (omitting steps 2 and 3 in Fig. 2), the ion exchange (omitting step 3) and the chemical reduction steps (no steps omitted). FTIR spectra of the samples annealed in each curing environment for 90 min immediately after the KOH imide ring cleavage step can be seen in Fig. 6.

Reimidization has not occurred at this stage in any of the curing environments, with the amide peaks (1650 cm^{-1} and 1550 cm^{-1}) clearly visible and the imide ring peaks (1780 cm^{-1} and 1710 cm^{-1}) much less pronounced than the untreated spectrum. This is notable as a temperature of 250 °C has previously been used to cure PEI [17] and is also well known to (re-)imidize PIs [8]. Since neither of these studies carried out reimidization with potassium ions present, an explanation could be that the potassium ions hinder the reimidization process, although this is not likely as reimidization does occur after the silver ion-exchange step in most cases (see Fig. 7).

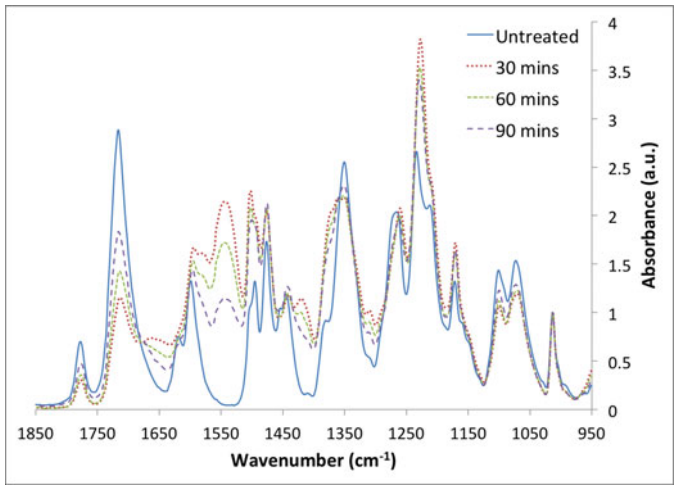

Fig. 8. FTIR spectra of PEI samples annealed in nitrogen atmosphere for various times after ion-exchange step.

These samples with unreduced silver ions showed a distinct color change, with the PEI becoming dark orange/brown much like PMDA-ODA PI, suggesting that a small degree of thermal reduction occurred. The curing environment can also be seen to have an effect. The color of the air and vacuum-cured samples were very similar with the nitrogen-cured samples exhibiting a less pronounced color change. This effect can be partially explained by comparing their FTIR spectra as shown in Fig. 7. Again, in this figure, 30 and 60 min anneal time samples are not shown for clarity. While all samples have substantially regained their imide peaks and lost the amide(I) peak, there is still a noticeable amide(II) peak (1550 cm^{-1}) in all samples, indicating that complete reimidization may not have occurred. Although these peaks in the air and vacuum-cured samples have decreased enough to be considered negligible, the peak in the nitrogen-cured samples remains prominent. The nitrogen curing environment over differing times (see Fig. 8) indicates that reimidization is occurring, but at a more gradual pace than the air and vacuum atmospheres.

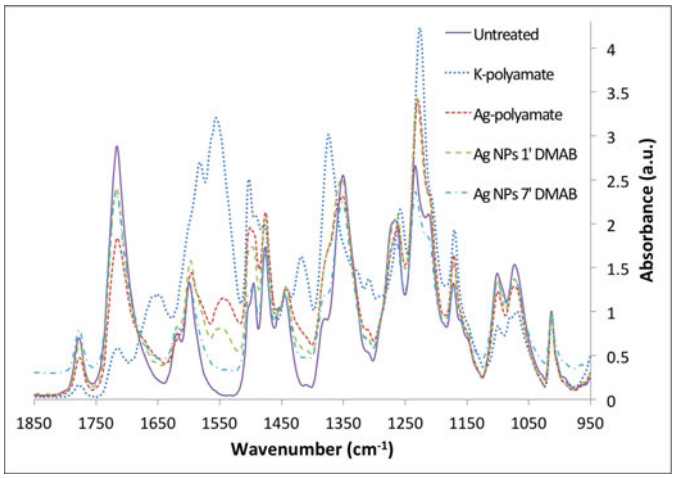

Fig. 9. FTIR spectra of PEI samples annealed for 90 min in nitrogen atmosphere after each process step.

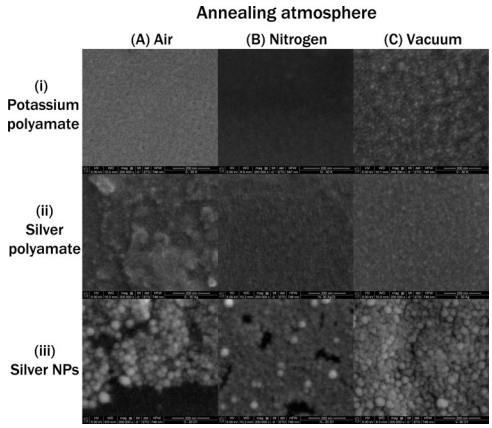

Fig. 10. FESEM of the samples annealed for 90 min in different atmospheres after (i) process step 1 in Fig. 2, (ii) step 2, and (iii) after step 3. Scale bar is 200 nm.

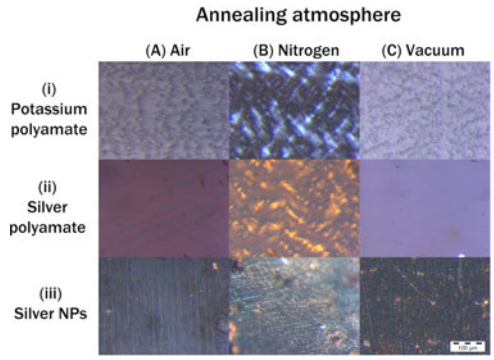

Fig. 11. Microscope images of the samples annealed for 90 min in different atmospheres after (i) process step 1 in Fig. 2, (ii) step 2, and (iii) after step 3. Scale bar is 100 μm.

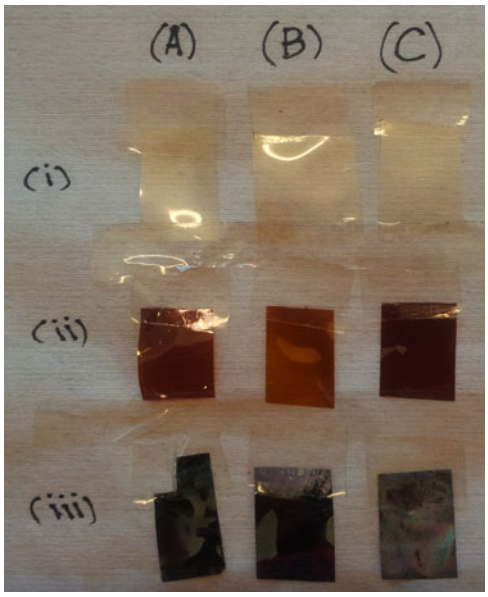

Fig. 12. Photographic image of samples shown in Figs. 10 and 11 above. Sample sizes are approximately 2 cm $\times$ 3 cm.

It also appears that the presence of silver nanoparticles has an effect on reimidization, accelerating the process. This effect has been previously been observed and characterized by Qi *et al*. [25]. Fig. 9 shows the FTIR spectra from the samples cured for 90 min in a nitrogen atmosphere. Each plot represents a measurement taken after each process step with two taken after the silver ion reduction step; one with a DMAB immersion time of 1 min and a second with an immersion time of 7 min. This suggests that the silver nanoparticles may have a positive effect on reimidization, possibly due to the added thermal conductance of the silver around the polymer chains.

FESEM and microscope images of the substrates can be seen in Figs. 10 and 11, respectively. Clearly, the surface morphology and formation of the silver nanoparticles depend strongly on the annealing atmosphere. Despite these images, FTIR analysis of the samples exposed to 7 min DMAB reduction and annealed for 90 min provided broadly similar results across the different annealing atmospheres (not shown). Although this indicates reimidization has occurred across all annealing atmospheres, the SEM images show different patterns of silver growth in the final row. The air- and vacuum-annealed samples seem to show good coverings of silver, with the vacuum-annealed sample showing greater uniformity. The nitrogen sample appears to show a reasonably densely packed layer of silver nanoparticles, with a few isolated, possibly detached, agglomerations on top of this.

Figs. 11 and 12 show that all three annealing environments produce a largely continuous layer of silver although the morphologies are different. Before reduction of the silver ions, the nitrogen-cured samples appear to have a much greater difference in surface texture [B (i) and (ii) compared to A/C (i) and (ii)].

The photograph in Fig. 12 shows the same samples seen in Figs. 10 and 11. Clearly this indicates the changes occurring at each stage of the process, with all DMAB-treated samples showing a definite silver color. The vacuum-cured sample [C (iii)] appears slightly whiter. This white form of silver is similar to electrolessly plated silver as previously reported by the group [26], but not present in high enough concentration to be conductive.

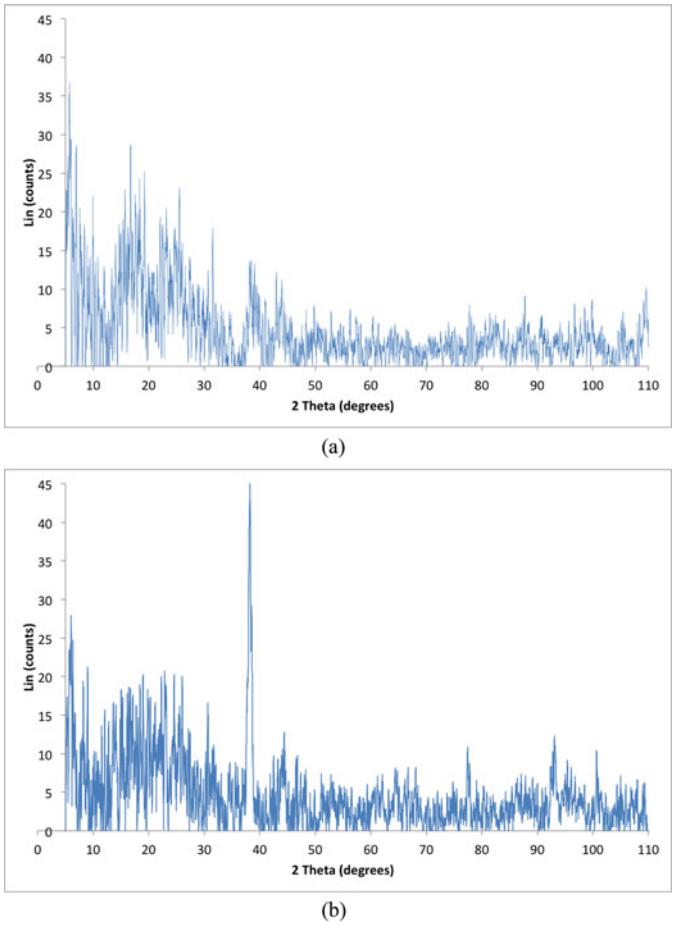

Fig. 13. XRD samples of PEI with (a) ion exchange only with no chemical reduction and (b) chemically reduced silver nanoparticles.

Finally, XRD measurements were taken to confirm the presence of reduced, metallic silver. Fig. 13(a) shows the diffraction pattern from a PEI sample that has been the subject of the ion-exchange process but no reduction has taken place. No crystalline diffraction peaks can be discerned to stand out from the noise level, indicating a purely amorphous sample. Fig. 13(b) shows a sample cured in a vacuum environment for 30 min after a DMAB reduction time of 7 min. A crystalline peak at 38.2° is clearly seen, and also peaks at 45° and 77° in this DMAB-reduced sample (final row, third column of Fig. 10). These coincide with the Ag diffraction peaks (111), (200), and (311), respectively [27], confirming the presence of crystalline silver. The lack of prominence of the peaks can be attributed to the low volume fraction of silver in the sample. The samples cured in a nitrogen atmosphere exhibited the largest peaks with the air-cured samples providing only slightly smaller peaks than the vacuum-annealed samples. Although the difference is not large, it suggests either that the absence of oxygen has a positive effect on *in-situ* silver nanoparticle formation and that the vacuum environment somehow retards silver growth or that silver oxide is formed, which does not exhibit the same peaks as pure silver.

The diffraction peak at 38.2° [see Fig. 13(b)] also allows an estimate of the average crystalline correlation length for the silver crystals, τ, to be made using the Scherrer formula [28]:

$$\tau = \frac{K\lambda}{\beta \cos\theta} \tag{1}$$

where K is the dimensionless shape factor (≈1), λ is the X-ray wavelength (1.5418 Å), β is the full width half maximum of the peak value in radians (7.4×10^{-3}), and θ is the Bragg angle (19°). This estimate gives a mean silver crystal size of approximately 20 nm, which agrees well with the SEM images in row (iii) of Fig. 10, giving a silver nanoparticle size of approximately 20–30 nm. The silver nanoparticles may be composed of single crystals, but nanoparticles with more than one single crystal, or with crystalline defects, would be consistent with a lower crystalline correlation length.

V. Conclusion

This paper demonstrates alkaline hydrolysis of PEI, with temperature being the key factor in the reaction. Compared to PI, PEI is more resilient to this surface modification approach, requiring more severe experimental parameters to achieve full imide ring cleavage. Ion exchange of silver and potassium ions within the modified substrate and subsequent *in situ* reduction of the silver ions have also been demonstrated and experimentally verified. Although exploratory, this study offers interesting opportunities toward achieving direct metallization onto PEI, extending the scope of the group's novel fabrication process by providing a new substrate candidate. Despite the PEI monomer having the same number of cleavable imide rings as its Kapton counterpart, and therefore the same number of potential ion-exchange sites, it has a greater chain length per repeat unit such that it is not expected that similar densities of silver nanoparticles on the surface are achievable. It should however be sufficient to act as a catalytic seed layer for electroless plating. It is the aim of future work to investigate this and to characterize the metal deposits through conductivity measurements and also to selectively pattern the PEI to demonstrate its potential for circuit interconnection.

References

[1] IDTechEx, "Flexible electronics masterclass," in *Plastic Electronics Europe*, S. Reuter, Ed. Berlin, Germany: IDTechEx, 2012.

[2] R. E. Southward, C. M. Boggs, D. W. Thompson, and A. K. St. Clair, "Synthesis of surface-metallized polyimide films via in situ reduction of (perfluoroalkanoato)silver(i) complexes in a poly(amic acid) precursor," *Chem. Mater.*, vol. 10, no. 5, pp. 1408–1421, 1998.

[3] D. S. Thompson, L. M. Davis, D. W. Thompson, and R. E. Southward, "Single-stage synthesis and characterization of reflective and conductive silver polyimide films prepared from silver(i) complexes with ODPA/44,-ODA," *ACS Appl. Mater. Interfaces*, vol. 1, no. 7, pp. 1457–1466, 2009.

[4] K. Cheng, M. H. Yang, W. W. W. Chiu, C. Y. Huang, J. Chang, T. F. Ying, and Y. Yang, "Ink-jet printing, self-assembled polyelectrolytes, and electroless plating: Low cost fabrication of circuits on a flexible substrate at room temperature," *Macromol. Rapid Commun.*, vol. 26, no. 4, pp. 247–264, 2005.

[5] W. Cui, W. Lu, Y. Zhang, G. Lin, T. Wei, and L. Jiang, "Gold nanoparticle ink suitable for electric-conductive pattern fabrication using in ink-jet printing technology," *Colloids Surfaces A, Physicochem. Eng. Aspects*, vol. 358, no. 1–3, pp. 35–41, 2010.

[6] O. Dos Santos Ferreira, A. Stevens, and C. Schrauwen, "Quantitative comparison of adhesion in metal-to-plastic systems," *Thin Solid Films*, vol. 517, no. 10, pp. 3070–3074, 2009.

[7] S. Ikeda, K. Akamatsu, and H. Nawafune, "Direct photochemical formation of Cu patterns on surface modified polyimide resin," *J. Mater. Chem.*, vol. 11, no. 12, pp. 2919–2921, 2001.
[8] K. Akamatsu, S. Ikeda, and H. Nawafune, "Site-selective direct silver metallization on surface-modified polyimide layers," *Langmuir*, vol. 19, no. 24, pp. 10366–10371, 2003.
[9] J. H. G. Ng, M. P. Y. Desmulliez, M. Lamponi, B. G. Moffat, A. McCarthy, H. Suyal, A. C. Walker, K. A. Prior, and D. P. Hand, "A direct-writing approach to the micro-patterning of copper onto polyimide," *Circuit World*, vol. 35, no. 2, pp. 3–17, 2009.
[10] Y. Kato, K. Maki, S. Furukawa, and M. Kashino, "A photosensitive polyimide based method for an easy fabrication of multichannel neural electrodes," in *Proc. 30th Annu. Int. IEEE Eng. Med. Biol. Soc. Conf.*, Vancouver, BC, Canada, 2008, pp. 5802–5805.
[11] Y. Matsumura, Y. Enomoto, T. Tsuruoka, K. Akamatsu, and H. Nawafune, "Fabrication of copper damascene patterns on polyimide using direct metallization on trench templates generated by imprint lithography," *Langmuir*, vol. 26, no. 14, pp. 12448–12454, 2010.
[12] Q. Zhou, H. Chen, and Y. Wang, "Region-selective electroless gold plating on polycarbonate sheets by UV-patterning in combination with silver activating," *Electrochimica Acta*, vol. 55, no. 7, pp. 2542–2549, 2010.
[13] *Kapton HN Technical Data Sheet*, DuPont, Ed, Wilmington, DE, USA, 2011.
[14] P. J. Rousche, D. S. Pellinen, D. P. Pivin, Jr., J. C. Williams, R. J. Vetter, and D. R. kirke, "Flexible polyimide-based intracortical electrode arrays with bioactive capability," *IEEE Trans. Biomed. Eng.*, vol. 48, no. 3, pp. 361–371, Mar. 2001.
[15] S. Carroccio, C. Puglisi, and G. Montaudo, "Thermal degradation mechanisms of polyetherimide investigated by direct pyrolysis mass spectrometry," *Macromol. Chem. Phys.*, vol. 200, pp. 2345–2355, 1999.
[16] S. Carroccio, C. Puglisi, and G. Montaudo, "Photo-oxidation products of polyetherimide ULTEM determined by MALDI-TOF-MS. Kinetics and mechanisms," *Polym. Degradation Stability*, vol. 80, pp. 459–476, 2003.
[17] A. V. Gaikwad and T. K. Rout, "*In situ* synthesis of silver nanoparticles in polyetherimide matrix and its application in coatings," *J. Mater. Chem.*, vol. 21, pp. 1234–1239, 2011.
[18] S.-Y. Kim and K.-H. Lee, "Effects of chemical transition of polyetherimide membranes having an integrally skinned asymmetric structure," *Current Appl. Phys.*, vol. 9, pp. e51–e55, 2009.
[19] M. Eisenbarth and K. Feldmann, "Pressfit technology for 3-D molded interconnect devices (MID)—A lead-free alternative to solder joints—Challenges and solutions concepts," in *Proc. 27th Annu. IEEE/SEMI Int. Electron. Manuf. Technol. Symp.*, 2002, pp. 238–244.
[20] J. H. G. Ng, M. P. Y. Desmulliez, K. A. Prior, and D. P. Hand, "Ultraviolet direct patterning of metal on polyimide," *Micro Nano Lett.*, vol. 3, no. 3, pp. 82–89, 2008.
[21] J. H. G. Ng, D. E. Watson, J. Sigwarth, A. McCarthy, K. A. Prior, D. P. Hand, W. Yu, R. W. Kay, C. Liu, and M. P. Y. Desmulliez, "On the use of silver nanoparticles for direct micropatterning on polyimide substrates," *IEEE Trans. Nanotechnol.*, vol. 11, no. 1, pp. 139–147, Jan. 2012.
[22] H. Okumura, T. Takahagi, N. Nagai, and S. Shingubara, "Depth profile analysis of polyimide film treated by potassium hydroxide," *J. Polym. Sci. B, Polym. Phys.*, vol. 41, pp. 2071–2078, 2003.
[23] Y.-S. Hsiao, W.-T. Whang, S.-C. Wu, and K.-R. Chuang, "Chemical formation of palladium-free surface-nickelized polyimide film for flexible electronics," *Thin Solid Films*, vol. 516, pp. 4258–4266, John Wiley, 2008.
[24] J. Coates, *IR Spectra Interpretation: A Practical Approach*. New York, NY, USA: Wiley, 2000.
[25] S. Qi, Z. Wu, D. Wu, W. Yang, and R. Jin, "The chemistry involved in the loading of silver (I) into poly (amic acid) via ion exchange: A metal-ion-induced crosslinking behavior," *Polymer*, vol. 50, no. 3, pp. 845–854, 2009.
[26] D. E. Watson, J. H. G. Ng, and M. P. Y. Desmulliez, "Additive photolithography based process for metal patterning using chemical reduction on surface modified polyimide," in *Proc. 18th Eur. Microelectron. Packag. Conf.*, 2011, pp. 1–7.
[27] JCPDS, card 4-0783 (Standard silver crystal). International Centre for Diffraction Data. Available: www.icdd.com.
[28] A. L. Patterson, "The scherrer formula for x-ray particle size determination," *Phys. Rev.*, vol. 56, no. 10, pp. 978–982, 1939.

David E. Watson was born in Aberdeen, Scotland, U.K. He received the B.Eng. degree in electronic and software engineering from Aberdeen University, Aberdeen, U.K., in 2005, and the M.Sc. degree in microsystems engineering from Heriot-Watt University, Edinburgh, U.K., in 2008, where he is currently working toward the Ph.D. degree in microsystems in the MISEC group.

His main research interests include flexible electronics, microelectromechanical systems packaging, and microfluidic systems.

Jack H.-G. Ng was born in Hong Kong and has lived in Scotland since childhood. He received the B.Sc. (Hons.) degree in physics from the University of Edinburgh, Edinburgh, U.K. where he developed interests in micro/nanoscale sciences, and the M.Sc. (by research) degree in nanomaterials from the University of Central Lancashire, Preston, U.K. He received the Ph.D. degree on the "Development of a Direct Metallization for Micro-engineering" at the Microsystems Engineering Centre, Heriot-Watt University, Edinburgh, U.K., in 2012

He is currently a Postdoctorate Research Associate at Heriot-Watt University. His research interests include deposition and patterning of metals on nonconducting surfaces, particularly metal nanoparticles, wet chemical surface modification, electroless plating, upscale manufacturing, laser direct-write applications, flexible electronics, and packaging of medical devices.

Knut E. Aasmundtveit (M'06) received the M.Sc. degree in technical physics from the Norwegian Institute of Technology, Trondheim, Norway, in 1994, and the Ph.D. degree in materials physics from the Norwegian University of Science and Technology, Trondheim, in 1999.

He is a Professor at the Department of Micro and Nano Systems Technology (IMST), Buskerud and Vestfold University College (HBV) Norway. His research interests and teaching activities include packaging and integration technology for micro- and nanosystems such as intermetallic and polymer-based bonding, nanomaterials integration in microsystems, and biomedical packaging. He was with Alcatel Space Norway/Ame Space (now Kongsberg Norspace), Horten, Norway, as Radio Frequency System Design Engineer, until 2004, when he joined HiVe-IMST as an Associate Professor, becoming Professor in 2013. He has authored or coauthored four book chapters and more than 70 journal and conference papers.

Marc P. Y. Desmulliez (M'08–SM'12) was born in Lille, France, in 1963. He received the Graduate degree from the Ecole Superieure d'Electricite of Paris, Paris, France, in 1987. He received two College Diplomas in microwave and modern optics from University College London, London, U.K., and in theoretical physics from the University of Cambridge, Cambridge, U.K., in 1987 and 1989, respectively. He received the Ph.D. degree in optoelectronics from Heriot-Watt University, Edinburgh, U.K., in 1995.

He is currently the Head of the Research Institute of Signals, Sensors and Systems in the School of Engineering & Physical Sciences at Heriot-Watt University, and has been directing the Microsystems Engineering Centre since 1999. This Centre regroups six academic members of staff and more than 30 Ph.D. students and Researchers specialized in all aspects of microelectromechanical systems (MEMS) manufacturing packaging, and testing. His major fields of study are MEMS, advanced packaging, microwave sensing, and manufacturing technologies where he has coauthored more than 340 publications and held nine patents. His current research interests include the post-CMOS processing of MEMS and advanced 3-D manufacturing technologies.

Dr. Desmulliez is a Fellow of the Institute of Engineering and Technology and a Fellow of Institute of Physics. He is a Chartered Engineer and a Chartered Physicist from the U.K. Institute of Physics.